Characterizing the Mechanical Properties of Solvent-Cast 3D-Printed Biodegradable Polymer Constructs

Juan P. Mendoza[1], Andrew Kitson[1], Santiago Lazarte[2], Brandon A. Krick[3], Lesley W. Chow[1,4]

[1]Department of Materials Science and Engineering, Lehigh University, Bethlehem, PA, USA and [2]Department of Chemical and Biomedical Engineering, Florida A&M University, Tallahassee FL, USA
[3]Department of Mechanical Engineering, Florida A&M University-Florida State University, Tallahassee, FL, USA and [4]Department of Bioengineering, Lehigh University, Bethlehem, PA, USA

Introduction

- Physical properties of biomaterials are critical in driving cell-material interactions[1,2]
- Changes in cellular responses due to scaffold architecture and mechanical properties are difficult to decouple
- Our preliminary data showed that lower porosity promoted human mesenchymal stromal cell (hMSC) osteogenesis while higher porosity enhanced both chondrogenesis and osteogenesis
- We hypothesize that this effect is caused by differences in scaffold stiffness due to changes in scaffold porosity
- The goal of this work is to characterize poly(caprolactone) (PCL) scaffolds printed with different porosities to investigate how architecture affects scaffold stiffness (**Fig. 1**)

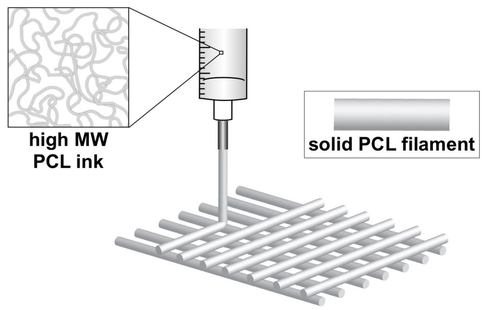

Figure 1. PCL is dissolved at 370 mg/mL in a volatile solvent (hexafluoroisopropanol; HFIP) and extruded through a nozzle. HFIP evaporates, leaving behind a solid PCL filament.

Solvent-Cast 3D printing

- Inks were extruded through a 32G (100 µm inner diameter) needle using a Nordson EV Fluid Dispensing Robot (**Fig. 2**)
- Scaffolds (N=3 inks per group) were printed with different filament spacing (FS): 190 µm, 260 µm, and 400 µm

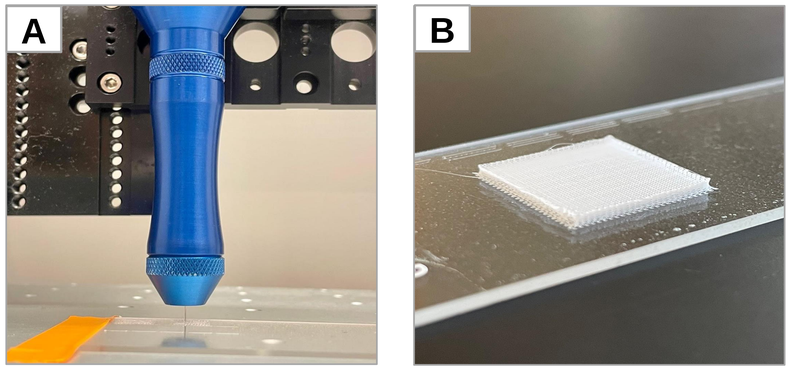

Figure 2. Scaffolds were printed using the same overall dimensions (15 mm x 15 mm x 24 layers) and print parameters (pressure: 70 psi; line speeds: 0.4 mm/s (first layer) and 0.2 mm/s (subsequent layer); layer spacing: 45 µm). Each scaffold was printed using an offset architecture where every other layer is shifted in the X/Y direction by ½ its respective FS. **(A)** Nordson EV Fluid Dispensing Robot printer head. **(B)** Macroscopic image of solvent-cast 3D-printed scaffold.

Microindentation

- A 6-mm biopsy punch was used to cut multiple samples from each scaffold to obtain an average value for each ink
- Samples were fixed to a glass slide and quasistiatically compressed using a custom-built microindenter (**Fig. 3**)

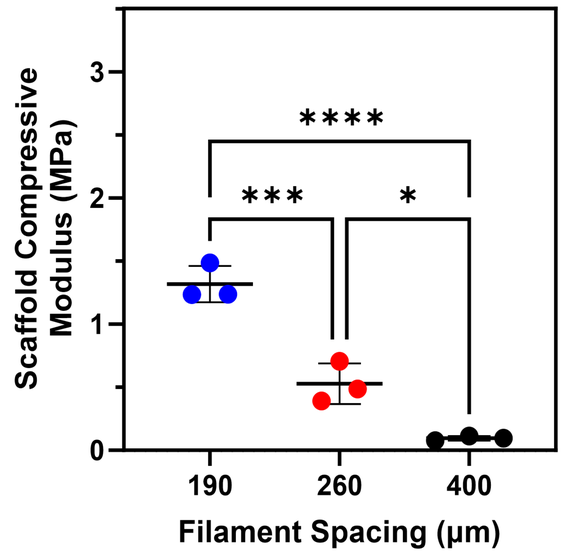

Figure 3. Compressive moduli of PCL scaffolds 3D printed with 190, 260, and 400 µm filament spacing. All groups were significantly different from each other. (N=3/group *p < .05; ***p < .001; ****p < .0001)

Scanning Electron Microscopy and Filament Characterization

- Scaffolds were imaged utilizing SEM to confirm scaffold architecture via filament diameter and spacing measurements (**Fig. 4, A-C**)
- Pore size and filament diameter were measured with ImageJ using 8 measurements per image and 5 SEM images per scaffold (N=3 inks per group) (**Fig. 4 D-E**)

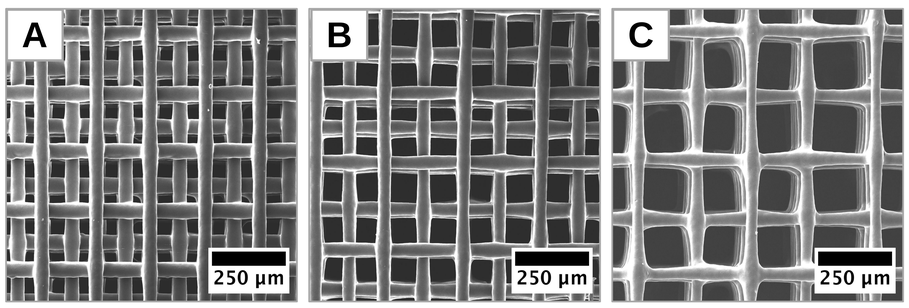

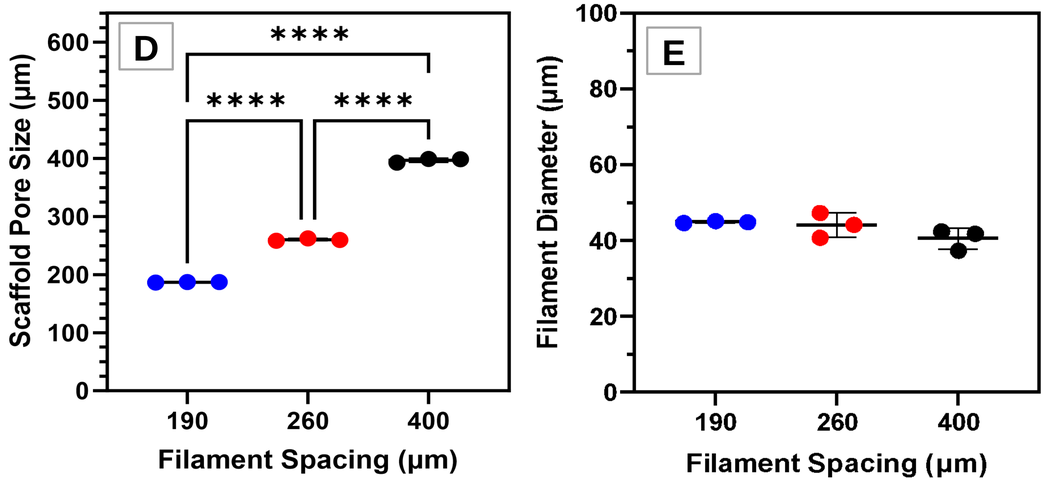

Figure 4. Representative SEM images of **(A)** 190, **(B)** 260, **(C)** 400 scaffolds. **(D)** Pore size and **(E)** filament diameter measurements. Pore sizes were statistically significant between all groups (N=3/group; ****p < .0001). We saw no statistical differences in filament diameter across groups.

Conclusions

- PCL scaffolds with different FS were successfully 3D printed and characterized using microindentation and SEM
- As expected, scaffolds with higher porosity showed lower compressive moduli while scaffolds with lower porosity had higher compressive moduli
- Filament diameters were consistent across all groups and pore sizes matched programmed values
- Future work includes culturing human mesenchymal stromal cells in these scaffolds under differentiation conditions to investigate how porosity affects osteogenic and chondrogenic activity

References: [1] Engler, A.J., et al. (2006). *Cell*, **126** (4), 677–689. [2] Discher, D.E., et al. (2005). *Science* (80-.)., **310** (5751), 1139–1143.

Acknowledgments: The authors acknowledge Lehigh's Electron Microscopy and Nanofabrication Facility and Institute for Functional Materials and Devices (I-FMD). This work was generously supported by the National Science Foundation (NSF) through a Faculty Early Career Development (CAREER) award (DMR 1944914 to LWC) and Graduate Research Fellowships (DGE 2234658 to AK). BAK and SL were supported by NSF CAREER award (CMMI 2027029 to BAK).